*Journal of Statistical Physics, Vol. 63, Nos. 3/4, 1991*

# Transmission of Waves by a Nonlinear Random Medium

**R. Knapp,[1] G. Papanicolaou,[2] and B. White[3]**

*Received October 17, 1990; final January 16, 1991*

We study analytically and numerically the effect of nonlinearity on transmission of waves through a random medium. We introduce and analyze quantities associated with the scattering problem that clarify the lack of uniqueness due to the nonlinearity as well as the localization of waves due to the random inhomogeneities. We show that nonlinearity tends to delocalize the waves and that for very large scattering regions the average transmitted energy is small.

**KEY WORDS:** Localization; nonlinear waves.

## 1. INTRODUCTION

In one-dimensional, linear random media the amount of energy transmitted by monochromatic waves is exponentially decreasing as a function of the size of the scattering region. This is one of the several manifestations of localization of waves in one-dimensional random media. In this paper we analyze the effect of nonlinearity on these phenomena.

We consider a simple model of monochromatic light waves propagating in a layered, nonlinear dielectric medium. Such a medium can have optical bistability whether or not there is randomness. An optical device is said to be bistable if two (or more) output states are possible for a given input state, depending on hysteresis. See Fig. 1. Bistable devices have many potential applications, since they can be used as direct optical switches.[9] This paper analyzes the effect of randomness on bistability.

As the length of the scattering region increases, so in general does the multiplicity of solutions. We therefore introduce the average multiplicity of

[1] Los Alamos National Laboratory, Los Alamos, New Mexico 87545.
[2] Courant Institute, 251 Mercer Street, New York, New York 10012.
[3] Exxon Research and Engineering Company, Route 22, East Annandale, New Jersey 08801.



0022-4715/91/0500-0567$06.50/0 

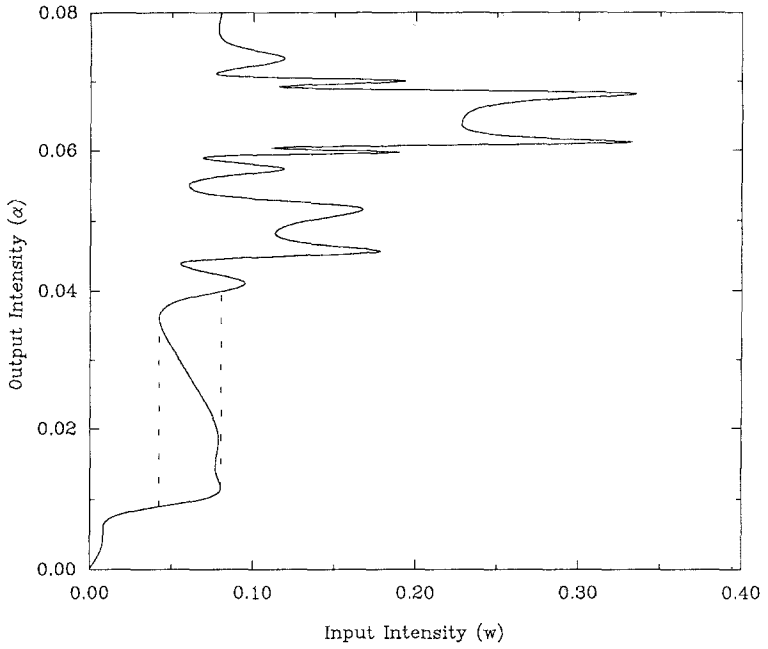


Fig. 1. Optical bistability. The dotted lines show the jumps the hysteresis curve would take if the input intensity $w$ were slowly increased and then slowly decreased in that region of the curve. The calculations were done from Eqs. (3) and (5) with $L = 300$ and $\varepsilon = 0.25$.

solutions with given transmittivity as a function of the strength of the nonlinearity and the size of the scattering region. In the linear case, localization implies that this quantity goes to zero as the size of the scattering region increases for any nonzero transmittivity. If the same happens in the nonlinear case, then we have localization of all solutions. In this paper we compute and analyze the properties the average multiplicity of solutions in the weakly nonlinear diffusion limit. In this limit the nonlinearity and randomness are small and the size of the scattering region is large.

We find that the average transmittivity increases with nonlinearity for a fixed scattering region, indicating that nonlinearity tends to delocalize the waves. We also find numerically that the average transmittivity decreases with the size of the scattering region for fixed nonlinearity. The decay rate of the average transmittivity is well known in the linear case. In the nonlinear case the average transmittivity goes to zero as the size of the scattering region increases, but we have not computed the decay rate in this paper.

Both bistability and localization are discussed in some detail in refs. 4 and 5. The equations and scaling we use are given in Section 2. In Section 3

we discuss the relation of our problem to the simpler fixed output problem discussed in refs 2 and 5 and elsewhere. Studies related to ours are presented in refs. 1, 3, and 10. In Section 4 we define the average multiplicity of solutions and the average transmittivity, which are the quantities of principal interest in this paper. In Section 5 we describe briefly the weakly nonlinear diffusion limit, which is well studied in the literature,[5,6,8] and analyze the behavior of the average transmittivity as the scattering region increases. In Section 6 we present the results of numerical simulations for both the original model equations and the limit equations.

To resolve the nonuniqueness of the time harmonic nonlinear scattering problem, we must go to a time-dependent formulation, which is not done in this paper. Many solutions of the time harmonic problem will be dynamically unstable, that is, unstable for the initial value problem, but they are nonetheless counted in the average multiplicity and transmittivity that we study here. Thus, while these quantities are useful analytical tools for studying nonlinear localization, they are not directly related to physical observables.

## 2. FORMULATION AND SCALING

We consider propagation of monochromatic light waves in a one-dimensional, nonlinear, and randomly inhomogeneous Fabry–Perot étalon of length $L$ with a wave incident form the right. If we take $x=0$ to be the left side of the medium, the equations for the (complex) scalar field amplitude $u$ are

$$\begin{aligned} u_{xx}+k^2n^2(x,|u|^2)u=0 \qquad & \text{for} \quad 0<x<L \\ u(x)=A_0(e^{-ikx}+Re^{ikx}) \qquad & \text{for} \quad x>L \\ u(x)=A_0Te^{-ikx} \qquad & \text{for} \quad x<0 \end{aligned}$$

Here $n$ is the index of refraction, $k$ is the wavenumber, $T$ and $R$ are the transmission and reflection coefficients, and $A_0$ is the incident wave amplitude. We restrict attention to a cubic nonlinearity and a small random perturbation so that

$$n^2(x,|u|^2)=1+\varepsilon\mu(x)+\tilde{w}\,|u|^2$$

Here $\tilde{w}$ is a material constant determined by the Kerr nonlinearity of the medium. We assume that $\mu$ is a stationary, ergodic process with correlation length $l$. The parameter $\varepsilon$ controls the size of the noise. Without noise and nonlinearity, $n\equiv 1$ and the medium is exactly matched to the adjoining space.

Since we are considering monocromatic waves, we can scale length by the wavelength. For simplicity we will use $L$ for $k$ times the length of the medium. We also scale the wave $u$ by the incident amplitude $A_0$. The resulting equation inside the medium is

$$u_{xx} + [1 + \varepsilon\mu(x) + w\,|u|^2]u = 0 \tag{1}$$

where $w = \tilde{w}\,|A_0|^2$ is proportional to the incident intensity. If we require the $u$ and $u_x$ to be continuous at the boundaries, then

$$\begin{aligned} u_x(0) + iu(0) &= 0 \\ u_x(L) - iu(L) &= -2ie^{-iL} \end{aligned} \tag{2}$$

which along with (1) is the scattering problem.

The transformation $u(x) = q(x)\,e^{i\gamma(x)}/|T|$ allows the boundary value problem (1, 2) to be converted into a family of initial value problems.[4,5] One reason for converting to an initial value problem is that solutions of the scattering problem are not unique in general; we have bistability. For the initial value problem the solution is unique and nonuniqueness arises from the algebraic problem of satisfying the boundary conditions. The equation for $\gamma$ can be solved in terms of $q$ and we get

$$q_{xx} - \frac{1}{q^3} + [1 + \varepsilon\mu(x)]q + \alpha q^3 = 0; \qquad q(0) = 1, \qquad q_x(0) = 0 \tag{3}$$

where $\alpha = w\,|T|^2$. Note that the parameter $\alpha$ is equal to the scaled output intensity. For a given fixed $\alpha$ we can solve (3) and determine the transmission coefficient and corresponding input intensity from the boundary condition at $x = L$,

$$|T|^2 = \frac{4}{q_x^2(L;\alpha) + q^2(L;\alpha) + 2 + 1/q^2(L;\alpha)} \tag{4}$$

$$w = \frac{\alpha}{|T|^2} = \frac{1}{4}\alpha\left[q_x^2(L;\alpha) + q^2(L;\alpha) + 2 + \frac{1}{q^2(L;\alpha)}\right] \tag{5}$$

We use this initial value formulation for numerical simulations of the scattering problem. In Section 5 we use a different initial value formulation with the same parameter $\alpha$ to compute quantities in the white noise limit.

## 3. FIXED INPUT AND FIXED OUTPUT

In the scattering problem it is natural to consider a specified input intensity. We would like to know the output state as a function of the input

state. When the output is fixed, then $\alpha$ is constant and we have the initial value problem (3), which is the fixed output problem.

In the linear case, where $\alpha = 0$, the two problems are equivalent because there is a unique output intensity for a given input intensity and vice versa. However, when there is bistability there could be several output intensities for a given input intensity. Figure 1 was generated by increasing the fixed output $\alpha$ in small steps to find the input $w$. It is clear from Fig. 1 that there can be no uniqueness of $|T|^2$ as a function of $w$.

Our goal is to solve the scattering problem in the random case using results from the initial value problem (3). For simplicity we will refer to the transmittivity by the variable $\tau$, so $|T|^2 = \tau$. Given a solution $q(L; \alpha)$ of (3), the solutions of the scattering problem are the fixed points of

$$\tau = \frac{4}{q_x^2(L; w\tau) + q^2(L; w\tau) + 1/q^2(L; w\tau) + 2} \tag{6}$$

In the linear case the solution is unique, since $q$ does not depend on $\alpha$, but in the general nonlinear case, there is little hope of finding all solutions to this problem.

## 4. AVERAGE MULTIPLICITY AND TRANSMITTIVITY

We have found that the statistical quantity which gives us the most information about localization or delocalization is the average density of solutions of Eq. (6) as a function of $\tau = |T|^2$, which we denote by $D(\tau; L, w)$. Let $N(\tau_1, \tau_2; L, w)$ be the expected number of solutions $\tau$ of (6) lying between $|T|^2 = \tau_1$ and $|T|^2 = \tau_2$. Then the average density of solutions is given by

$$D(\tau; L, w) = \lim_{\Delta\tau \to 0} \frac{N(\tau, \tau + \Delta\tau; L, w)}{\Delta\tau}$$

Clearly the total number of solutions is given by $N(0, 1; L, w) = \int_0^1 d\tau\, D(\tau; L, w)$. This is a measure of how likely bistability is in the nonlinear case. The density can also be used to find the average transmittivity defined by

$$\bar{\tau}(L, w) = \frac{\int_0^1 d\tau\, \tau D(\tau; L, w)}{\int_0^1 d\tau\, D(\tau; L, w)} \tag{7}$$

The average multiplicity density $D$ gives a lot of information about localization. When there is localization, the density function will have a peak near $\tau = |T|^2 = 0$ and most of the mass will be near zero. However, if

the peak is not near zero and the mass is spread out, it is no longer reasonable to say there is localization. Figure 5 shows two average multiplicity density functions, one indicating localization and one not.

We compute the average multiplicity density function using the Kac–Rice formula, which we recall briefly. Suppose the joint distribution of a random function $X(t)$ and its derivative with respect to $t$, $\dot{X}(t)$ is known. Then the expected number of zeros of $X(t)$ between $t_1$ ad $t_2$ is given by

$$\begin{aligned} N(t_1, t_2) &= E\left\{\int_{t_1}^{t_2} \delta(X(t))\,|\dot{X}(t)|\,dt\right\} \\ &= \int_{t_1}^{t_2} E\{\delta(X(t))\,|\dot{X}(t)|\}\,dt \\ &= \int_{t_1}^{t_2}\left[\int dx \int dy\, P_{X(t),\dot{X}(t)}(x, y)\,\delta(x)\,|y|\right] dt \\ &= \int_{t_1}^{t_2}\left[\int dy\, P_{X(t),\dot{X}(t)}(0, y)\,|y|\right] dt \end{aligned}$$

Let $X(\tau) = \tau - F(\tau)$, where $F(\tau)$ is the right-hand side of (6). Then the average density of solutions is simply given by the formula above with $t$ replaced by $\tau$ and stripped of the $t$ integral,

$$D(\tau; L, w) = \int dy\, P_{X(\tau),\dot{X}(\tau)}(0, y)\,|y| \tag{8}$$

Thus, to determine $D$, we need the joint distribution of $X(\tau)$ and $\dot{X}(\tau)$.

## 5. DIFFUSION LIMIT

We return to the boundary value problem (1), (2) and transform it as follows. We let

$$\begin{aligned} u &= Ae^{ix} + Be^{-ix} \\ u_x &= i(Ae^{ix} - Be^{-ix}) \end{aligned}$$

Then $A$ and $B$ satisfy the boundary value problem

$$\begin{aligned} A_x &= \frac{i}{2}(\varepsilon\mu + wC)(A + Be^{-2ix}) \\ B_x &= -\frac{i}{2}(\varepsilon\mu + wC)(Ae^{2ix} + B) \end{aligned} \tag{9}$$

with

$$C = |u|^2 = |A|^2 + |B|^2 + 2\,\mathrm{Re}(A\bar{B}e^{2ix})$$

and the boundary conditions

$$A(0) = 0, \qquad B(L) = 1$$

The reflection and transmission coefficients are given by

$$B(0) = T, \qquad A(L) = R$$

We convert the boundary value problem (9) into an initial value problem by replacing $A$ by $A/T$ and $B$ by $B/T$. Letting

$$\alpha = w\,|T|^2$$

we get

$$\begin{aligned} A_x &= \frac{i}{2}(\varepsilon\mu + \alpha C)(A + Be^{-2ix}) \\ B_x &= -\frac{i}{2}(\varepsilon\mu + \alpha C)(Ae^{2ix} + B) \end{aligned} \tag{10}$$

with

$$A(0) = 0, \qquad B(0) = 1$$

Then, with $\tau = |T|^2$ we have

$$\tau = \frac{1}{|B(L, \alpha)|^2}, \qquad w = \alpha\,|B(L, \alpha)|^2 \tag{11}$$

This is the parametric representation of the input–output problem; $w$ is the incident intensity, $\tau$ is the proportion of incident intensity transmitted, and $\alpha \geqslant 0$ is the parameter. Eliminating $\alpha$ leads to the fixed point equation

$$\tau = \frac{1}{|B(L, w\tau)|^2} \tag{12}$$

which is equivalent to (6).

The weakly nonlinear diffusion limit amounts to letting the size of the scattering region $L$ be large, $L = O(1/\varepsilon^2)$, and the incident intensity $w = O(\varepsilon^2)$. In this limit localization effects are fully developed in the linear case and bistability is present in a canonical way for the nonlinear deter-

ministic problem. Replacing $x$ by $x/\varepsilon^2$, $L$ by $L/\varepsilon^2$, $\alpha$ by $\varepsilon^2\alpha$, and $w$ by $\varepsilon^2 w$, we arrive at the scaled form of (10), (11),

$$\begin{aligned} A_x &= \frac{i}{2}\left(\frac{1}{\varepsilon}\mu\left(\frac{x}{\varepsilon^2}\right)+\alpha C\right)(A+Be^{-2ix/\varepsilon^2}) \\ B_x &= -\frac{i}{2}\left(\frac{1}{\varepsilon}\mu\left(\frac{x}{\varepsilon^2}\right)+\alpha C\right)(Ae^{2ix/\varepsilon^2}+B) \\ C &= |A|^2+|B|^2+2\,\mathrm{Re}(A\bar{B}e^{2ix/\varepsilon^2}) \\ A(0) &= 0, \qquad B(0)=1 \end{aligned} \tag{13}$$

The fixed point relation (12) remains the same in the scaled problem.

The limit of the process $(A, B)$ as $\varepsilon \to 0$ has been studied for a wide class of random coefficients $\mu$ in the linear case $\alpha = 0$.[6] When $\alpha$ is not zero the analysis is virtually identical and will not be repeated here. The main difference is that in order to calculate the average multiplicity of solutions $D$ for the fixed point equation (12) we need not only the limit law of $B$, but the joint limit law of $B(L, \alpha)$ and $B_\alpha = \partial B(L, \alpha)/\partial\alpha$, as we saw in (8). This means that we must get the limit law of $A$, $B$, $A_\alpha$, and $B_\alpha$. This is the main difference with the previous work.[6]

As in ref. 6, it is convenient to use polar coordinates. Noting that the solution of (13) satisfies

$$|B|^2 - |A|^2 = 1$$

we set

$$A = e^{-i(\phi+\psi)/2}\sinh\frac{\theta}{2}$$

$$B = e^{-i(\phi-\psi)/2}\cosh\frac{\theta}{2}$$

Then it is easy to see that $\theta$ and $\psi$ satisfy the equations

$$\begin{aligned} \theta_x &= -\left[\frac{1}{\varepsilon}\mu\left(\frac{x}{\varepsilon^2}\right)+\alpha\cosh\theta+\alpha\sinh\theta\cos\left(\psi-\frac{2x}{\varepsilon^2}\right)\right] \\ &\quad\times\sin\left(\psi-\frac{2x}{\varepsilon^2}\right) \\ \psi_x &= -\left[\frac{1}{\varepsilon}\mu\left(\frac{x}{\varepsilon^2}\right)+\alpha\cosh\theta+\alpha\sinh\theta\cos\left(\psi-\frac{2x}{\varepsilon^2}\right)\right] \\ &\quad\times\left[1+\cos\left(\psi-\frac{2x}{\varepsilon^2}\right)\coth\theta\right] \end{aligned} \tag{14}$$

and $\phi$ decouples and need not be considered. The initial conditions are $\theta(0, \alpha) = 0$ and $\psi$ need not be given initially because of the singular form of the equations. The fixed point equation in polar coordinates has the form

$$\tau = \frac{2}{1 + \cosh \theta(L, w\tau)} \tag{15}$$

We need therefore to determine the limit law of $\theta(L, \alpha)$ and $\theta_\alpha(L, \alpha)$ as $\varepsilon \to 0$. If $P$ is the joint density of $\theta$ and $\theta_\alpha$ in the limit, then the average density of solutions is given by

$$\begin{aligned} D(\tau; L, w) &= \iint d\theta \, d\theta_\alpha \, P(\theta, \theta_\alpha; L, w\tau) \, \delta\left(\tau - \frac{2}{1 + \cosh \theta}\right) \\ &\quad \times \left| 1 + \frac{2w\theta_\alpha \sinh \theta}{(1 + \cosh \theta)^2} \right| \\ &= \int d\theta_\alpha \, P\left(\cosh^{-1}\left(\frac{2}{\tau} - 1\right), \theta_\alpha; L, w\tau\right) \left| \frac{1}{\tau(1-\tau)^{1/2}} + \theta_\alpha w \right| \end{aligned} \tag{16}$$

To determine the asymptotic limit of $\theta$ and $\theta_\alpha$ as $\varepsilon \to 0$ we must analyze (14) along with equations for $\theta_\alpha$ and $\psi_\alpha$ the same way as in ref. 6 or ref. 8. The equations for $\theta_\alpha$ and $\psi_\alpha$ for $\varepsilon > 0$ are obtained from (14) by simply differentiating with respect to $\alpha$, so we will not write them out. We will also not show in detail the derivation of the limit diffusion process, since that is amply discussed in the above references and in ref. 5. We simply write the generator of the limit process, which is

$$\begin{aligned} \mathscr{L} = R_c \Bigg[ & \frac{\partial^2}{\partial \theta^2} + \operatorname{csch}^2 \theta \, \frac{\partial^2}{\partial \theta^2} + \psi_\alpha^2 \frac{\partial^2}{\partial \theta_\alpha^2} + (\theta_\alpha^2 \operatorname{csch}^4 \theta + \psi_\alpha^2 \coth^2 \theta) \frac{\partial^2}{\partial \psi_\alpha^2} \\ & - 2\psi_\alpha \coth \theta \, \frac{\partial^2}{\partial \theta \, \partial \psi_\alpha} - 2\theta_\alpha \psi_\alpha \operatorname{csch}^2 \theta \, \frac{\partial^2}{\partial \theta_\alpha \, \partial \psi_\alpha} \\ & + \coth \theta \, \frac{\partial}{\partial \theta} - \theta_\alpha \operatorname{csch}^2 \theta \, \frac{\partial}{\partial \theta_\alpha} \Bigg] - \frac{3}{2} (\alpha \theta_\alpha \sinh \theta + \cosh \theta) \frac{\partial}{\partial \psi_\alpha} \end{aligned} \tag{17}$$

Here $R_c$ is defined by

$$R_c = \frac{1}{2} \int_0^\infty R(s) \cos(2s) \, ds$$

$$R(s) = E\{\mu(s) \, \mu(0)\}$$

and is a positive constant. Since we are only interested in the law of $\theta$ and $\theta_\alpha$ we have dropped terms that involve $\psi$ in (17) since they decouple from the rest in the limit. The probability density of $\theta$, $\theta_\alpha$, and $\psi_\alpha$ is the solution of the Fokker–Planck equation

$$\frac{\partial P}{\partial x} = \mathscr{L}^* P \tag{18}$$

with $\mathscr{L}^*$ the (suitably defined) adjoint of $\mathscr{L}$.

From the form of the generator for $\theta$, $\theta_\alpha$, and $\psi_\alpha$ we see that it is not easy to get a feeling for how these processes behave. It is useful to note, however, that $\theta$, $\theta_\alpha$, and $\psi_\alpha$ are solutions of the Itô stochastic differential equations

$$\begin{aligned} d\theta &= R_c \coth\theta\, dx + (2R_c)^{1/2}\, dw_1 \\ d\theta_\alpha &= -R_c\theta_\alpha \operatorname{csch}^2\theta\, dx + (2R_c)^{1/2}\psi_\alpha\, dw_2 \\ d\psi_\alpha &= -\tfrac{3}{2}R_c(\alpha\theta_\alpha \sinh\theta + \cosh\theta)\, dx \\ &\quad - (2R_c)^{1/2}(\psi_\alpha \coth\theta\, dw_1 + \theta_\alpha \operatorname{csch}^2\theta\, dw_2) \end{aligned} \tag{19}$$

where $w_1$ and $w_2$ are independent, standard Brownian motions. Note that $\theta$ decouples from $\theta_\alpha$ and $\psi_\alpha$ and is simply the radial part of Brownian motion on the hyperbolic disk.[6]

When $w=0$ it is easy to see that $D(\tau; L, 0)$ behaves like the probability density of $\tau = |T|^2$ in the diffusion limit computed in ref. 6. The mean transmittivity at $w=0$ is

$$\bar{\tau}(L, 0) = \frac{4e^{-R_cL/4}}{\sqrt{\pi}} \int_0^\infty \frac{\eta^2 e^{-\eta^2}\, d\eta}{\cosh[\eta(R_cL)^{1/2}]} \tag{20}$$

which is formula (7.13) in ref. 6. As $L$ tends to infinity, we have

$$\bar{\tau}(L, 0) \sim \frac{\pi^{5/2} e^{-R_cL/4}}{2(R_cL)^{3/2}} \tag{21}$$

When the nonlinearity is not zero the mean transmittivity is given by

$$\begin{aligned} \bar{\tau}(L, w) = &\left\{ \iint d\theta\, d\theta_\alpha\, P\left(\theta, \theta_\alpha; L; \frac{2w}{1+\cosh\theta}\right) \frac{2}{1+\cosh\theta} \left| 1 + \frac{2w\theta_\alpha \sinh\theta}{(1+\cosh\theta)^2} \right| \right\} \\ &\times \left\{ \iint d\theta\, d\theta_\alpha\, P\left(\theta, \theta_\alpha; L; \frac{2w}{1+\cosh\theta}\right) \left| 1 + \frac{2w\theta_\alpha \sinh\theta}{(1+\cosh\theta)^2} \right| \right\}^{-1} \end{aligned} \tag{22}$$

which follows from (7) and the first line in (16). In Fig. 8 we plot $\bar{\tau}$ as a function of $L$ for different values of $w$ and we see that indeed the average transmittivity increases with $w$ for a fixed scattering region.

In the nonlinear case where $w$ is positive the denominator in (22) goes to infinity as $L$ increases, as seen in Fig. 6. Therefore, the large-$L$ behavior of $\bar{\tau}(L, w)$ for $w > 0$ cannot possibly be like the linear case (21). One might think that is true because once the fields become small deep inside the scattering region, the linear theory takes over and hence we have localization. However, as $L$ increases, more solutions are created and they localize at an even larger $L$. All this is contained in $\bar{\tau}(L, w)$, which is a statistical average and an average over all solutions. Its large-$L$ behavior is not known.

## 6. NUMERICAL SIMULATIONS

We have used numerical simulations in both the limit and finite-$\varepsilon$ case to explore the theory and to understand the range of its validity.

In the $\varepsilon \to 0$ limit we will study $D$ and $\bar{\tau}$ by simulating numerically the limit Itô equations (19). We do not solve the Fokker–Planck equation because it is too high-dimensional to easily solve and it has singularities.

Note that the Itô equations (19) are singular at the initial condition $\theta(0) = 0$. This is actually a removable singularity arising from the polar coordinates. If we use Cartesian coordinates

$$u = \tanh\frac{\theta}{2}\cos\psi \qquad \text{and} \qquad v = \tanh\frac{\theta}{2}\sin\psi$$

we can use the same process as before and get Itô equations

$$\begin{aligned}
du &= \left(\frac{R_c}{2}\right)^{1/2}(1-r^2)\,d\beta_1 \\
dv &= \left(\frac{R_c}{2}\right)^{1/2}(1-r^2)\,d\beta_2 \\
du_\alpha &= \frac{3}{2}v\left(\frac{1+r^2}{1-r^2}+4\alpha\frac{uu_\alpha+vv_\alpha}{(1-r^2)^2}\right)dx-(2R_c)^{1/2}\,(uu_\alpha\,d\beta_1+vu_\alpha\,d\beta_2) \\
dv_\alpha &= -\frac{3}{2}u\left(\frac{1+r^2}{1-r^2}+4\alpha\frac{uu_\alpha+vv_\alpha}{(1-r^2)^2}\right)dx-(2R_c)^{1/2}\,(uv_\alpha\,d\beta_1+vv_\alpha\,d\beta_2)
\end{aligned} \tag{23}$$

where $r = (u^2+v^2)^{1/2}$. These equations are not singular near the origin. Since the $\theta$ process tends to grow (linearly) toward $\infty$ as $x \to \infty$, $r$ approaches 1. Even though $r < 1$, numerical stability problems arise in

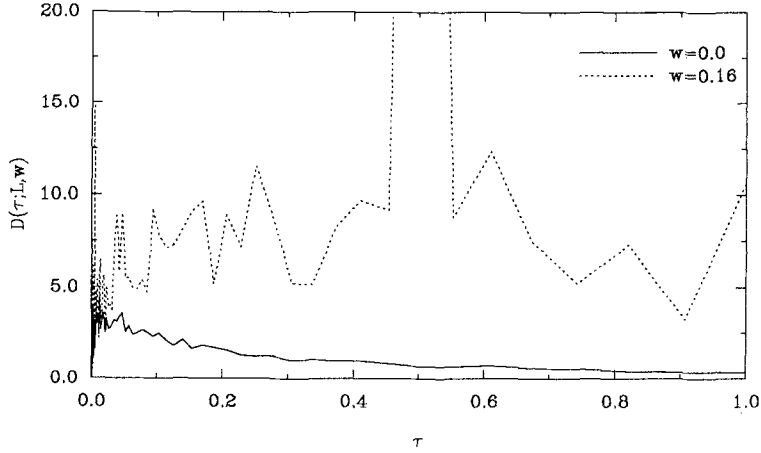


Fig. 2. Average density of solutions $D(\tau; L, w)$ as a function of transmittivity $\tau$ for $w = 0$ and $w = 0.16$ for $L = 30.0$. The density was compiled using 5000 realizations with $R_C \simeq 0.055$.

simulating Eqs. (23) when $r$ is near 1. To eliminate this problem, we started the simulations using a discrete analogue of Eqs. (23) and for $r > r_{\min}$ we used a hybrid system with $(u, v, \theta_\alpha, \psi_\alpha)$ to continue the calculation. In practice we got essentially the same results with the threshold in the range $0.25 < r_{\min} < 0.75$.

The results of the simulations for the limit process are shown in Figs. 2–4. Figure 2 shows the function $D(\tau; L, w)$ for $L = 30$ and $w = 0$ and $w = 0.16$. The solid curve for $w = 0$ has its peak and most of its mass near

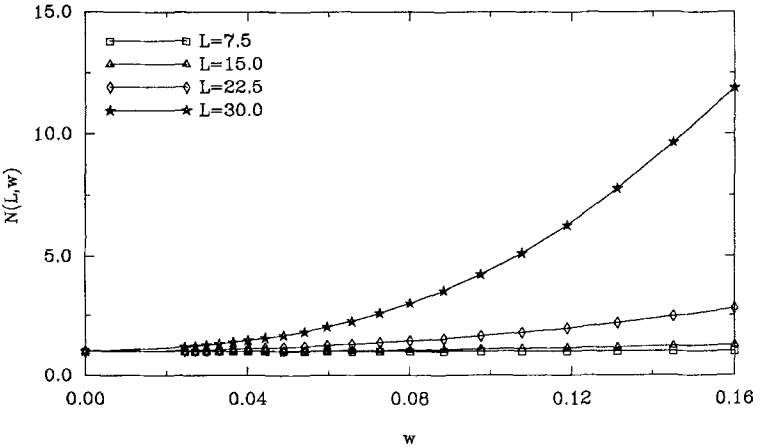


Fig. 3. Average multiplicity of solutions $N(0, 1; L, w)$ as a function of $w$ for $L = 7.5$, 15.0, 22.5, and 30.0. The averages are for 5000 realizations with $R_C \simeq 0.055$.

zero. This is an indication of localization. However, the mass for the dotted curve for $w = 0.16$ is shifted to the right from zero. Since we are simulating the white noise limit, there is a lot of fluctuation, so there appear to be many peaks in this curve, but if we were able to compute enough realizations, the curve would be much smoother. The shift of the curve to the right indicates delocalization in the nonlinear case. Notice also that the $w = 0.16$ curve is always higher than the one for $w = 0$. This is because in the nonlinear case there may be multiple solutions. The average multiplicity of solutions is quantified in Fig. 3, which shows $N(0, 1; L, w)$ as a function of $w$ for $L = 7.5$, 15.0, 22.5, and 30.0. These curves appear to be increasing exponentially fast, but we have not been able to carry the simulations out far enough to verify this. These curves can roughly be interpreted as predicting the likelihood of bistability. For example, if $N(0, 1; L, w) = 5$, a typical realization would have five possible solutions, or output states, for a given $L$ and $w$. (Not all of these would be stable, but it is necessary to solve the time-dependent problem to determine stability.) Figure 4 shows the weighted average transmittivity $\bar{\tau}$ as a function of $w$ for $L = 7.5$, 15.0, 22.5, and 30.0. Note that for the larger times, where localization was being felt in the linear case, these curves are increasing as a function of $w$. This is further evidence for delocalization for nonlinear wave propagation.

For comparison we also computed the average density of solutions directly from the equations for the initial value problem (3) with a positive $\varepsilon$. The code used for the positive $\varepsilon$ simulations is described in detail in ref. 5. The process $\mu$ is modeled by having constant values $\mu_i$ distributed

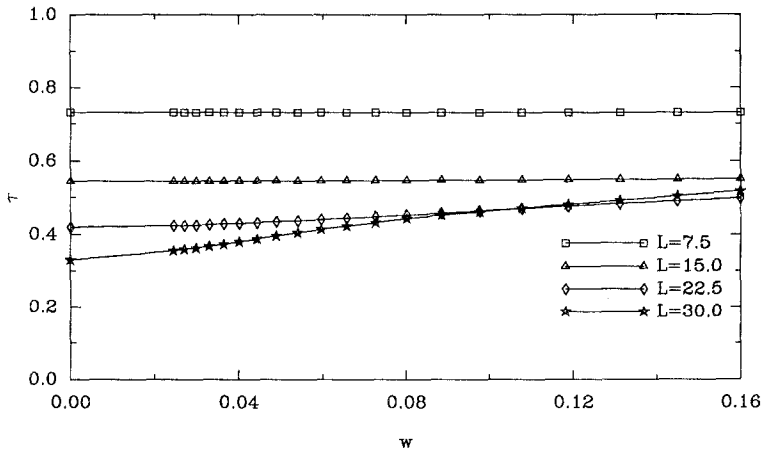


Fig. 4. Weighted average transmittivity $\bar{\tau}$ as a function of $w$ for $L = 7.5$, 15.0, 22.5, and 30.0. The averages are for 5000 realizations with $R_C \simeq 0.055$.

uniformly on $[-1, 1]$ over correlation intervals of constant correlation length $l$. Over each correlation interval the equation can be solved exactly using Jacobian elliptic functions. The result at the end of a correlation interval is then used as the initial condition for the next. To find the average number of roots and the function $F(\tau)$ we have for each realization of the random media traced the $\tau$ versus $w$ curve by using closely spaced values of $\alpha$ as in Fig. 1 [with the $\alpha$ axis transformed to $\tau$ using (4)]. As the curve is advanced, the solution is checked to see if it has crossed any of a given discrete set of $w$. When one of these values of $w$ has been crossed, the value of $\tau$ is stored in an appropriate bin. The density is approximated by finding the average number of $\tau$ values that lie in each bin for a given $w$ and $L$. In the results shown here we have used scaled values of the variables so that comparison with the limit theory is easier—i.e., we use $w = \text{physical } w/\varepsilon^2$ and $L = \text{physical } L\varepsilon^2$. We used a physical correlation length $l = 1.5$. Note, for example, that scaled $L = 30$ corresponds to a physical length $L = 480$, which is 320 slabs.

Figures 5–7 show the same quantities as Figs. 2–4, except that the results were found directly from the model equations with $\varepsilon = 0.25$. The results are qualitatively comparable to those for the limit $\varepsilon \to 0$. The physical $L$ and $w$ quantities were chosen so that they matched the scaled $L$ and $w$ quantities in the limit calculations.

The graphs for the weighted average transmittivity $\bar{\tau}$ agree very closely qantitatively. The density functions, however, do not match nearly so closely. It is readily apparent that the fluctuations for the limit equations are significantly larger. The curves would be closer if we had done the

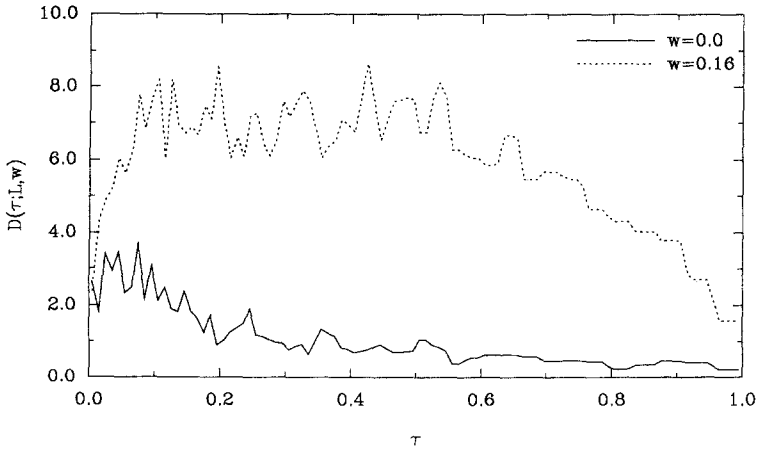


Fig. 5. Average density of solutions $D(\tau; L, w)$ as a function of transmittivity $\tau$ for $w = 0$ and $w = 0.10$ for $L = 30$. The density was compiled using 1000 realizations with $\varepsilon = 0.25$.

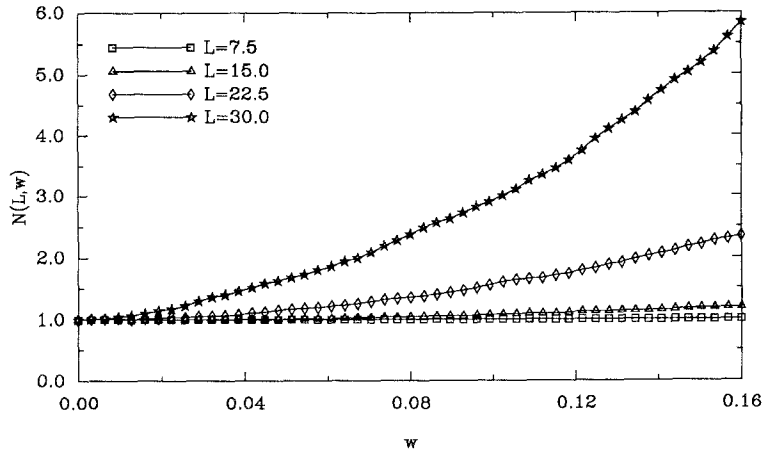


Fig. 6. Average multiplicity of solutions $N(0, 1; L, w)$ as a function of $w$ for $L = 7.5$, 15.0, 22.5, and 30.0. The averages are for 1000 realizations with $\varepsilon = 0.25$.

direct simulations with a smaller $\varepsilon$, but this was not practical, since the computation time increases quickly as $\varepsilon$ is reduced due to the $L = O(\varepsilon^2)$ scaling and the increase in fluctuations. The most important property we see in the density function for $w > 0$—that the mass of the curve is shifted significantly to the right—is seen for both simulations. The curves of $N(0, 1; L, w)$ as a function of $w$ have the same shape for the two different simulations, but the sizes differ. This is also due to the fluctuations. The

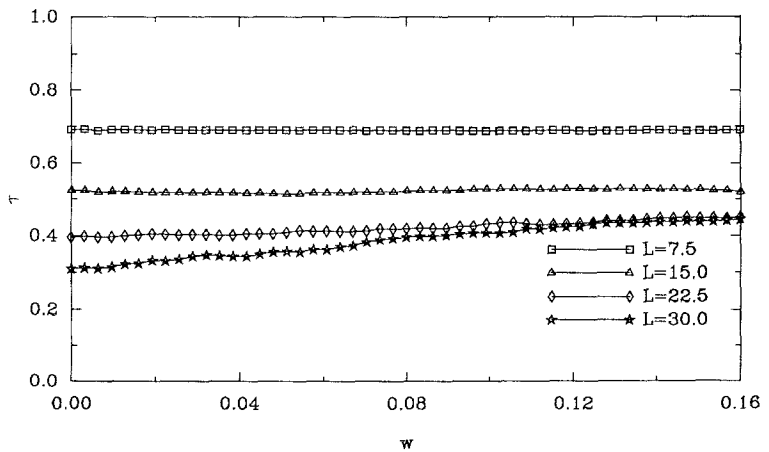


Fig. 7. Weighted average transmittivity $\bar{\tau}$ as a function of $w$ for $L = 7.5$, 15.0, 22.5, and 30.0. The averages are for 1000 realizations with $\varepsilon = 0.25$.

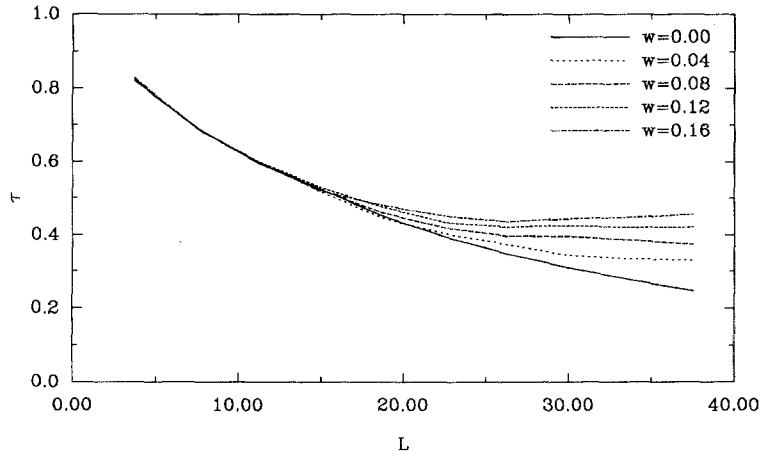


Fig. 8. Weighted average transmittivity $\bar{\tau}$ as a function of $x$ for $w = 0.0$, 0.04, 0.08, 0.12, and 0.16. The averages are for 1000 realizations with $\varepsilon = 0.25$.

graphs of the weighted average transmittivity match since by weighting we have canceled out the effects of the larger fluctuations.

Figure 8 provides a direct comparison of the decay of the weighted average transmittivity for the linear and nonlinear cases. The solid curve represents the exponential decay of the linear localization. For small $L$, $\bar{\tau}$ is nearly identical for the linear and nonlinear cases. In this regime nonlinear effects are not strong and there is no bistability. However, above some $L$, the decay slows for the nonlinear cases and eventually appears to stop. This indicates that there are a significant number of states which are delocalized.

The results we have shown here give strong evidence that there exist delocalized transmission states for the propagation of waves through a random medium. However, since we have only considered the time harmonic problem, not all of these states are physical. A complete study with a time-dependent model needs to be done to fully understand this issue.

## REFERENCES

1. G. I. Babkin and V. I. Klyatskin, Theory of wave propagation in nonlinear inhomogeneous media, *Sov. Phys. JETP* (1980).
2. P. Devillard and B. Souillard, Polynomially decaying transmission for the nonlinear schrödinger equation in a random medium, *J. Stat. Phys.* **43** (1986).
3. V. I. Klyatskin and E. V. Yaroshchuk, Numerical solution of the one dimensional problem of self-interaction of a wave in a layer of nonlinear medium, *Izv. Vyssh. Uchebn. Zaved. Radiofiz.* **28**(3) (1985).

4. R. Knapp, G. Papanicolaou, and B. White, Nonlinearity and localization in one dimensional random media, in *Disorder and Nonlinearity*, A. R. Bishop, D. K. Campbell, and S. Pnevmaticos, eds. (Springer, 1989), pp. 2–26.
5. R. J. Knapp, Nonlinearity and localization in one dimensional random media, Ph.D. thesis, New York University (1988).
6. W. Kohler and G. Papanicolaou, Power statistics for wave propagation in one dimension and comparison with transport theory, *J. Math. Phys.* **14**:1733–1745 (1973); **15**:2186–2197 (1974).
7. J. V. Maloney and A. C. Newell, Nonlinear optics, *Physica D*, to appear.
8. G. C. Papanicolaou, Asymptotic analysis of stochastic equations, in *Mathematical Association of America Studies in Mathematics*, Vol. 18, M. Rosenblatt, ed. (Mathematical Association of America, 1978).
9. M. E. Warren, S. W. Koch, and H. M. Gibbs, Optical bistability, logic gating, and waveguide operation in semiconductor etalons, *IEEE Computer* **20**(12):68–81 (1987).
10. I. O. Yaroshchuk, Numerical modeling of one dimensional problem of self-action of a wave in a stochastic nonlinear medium, *Izv. Vyssh. Uchebn. Zaved. Radiofiz.* **31**(1) (1988).